Eu(III) Luminescence Phase-Modulation Spectroscopy as a Site-Selective Probe of Y Zeolite

Hanshin Hwang, Sunbae Lee, and Du-Jeon Jang*

Department of Chemistry and Research Institute of Molecular Sciences, Seoul National University, Seoul 151-742, Korea
Received January 8, 1998

Phase shift spectroscopy is applied to Eu(III) luminescence from Eu^{3+}-exchanged Y zeolite. The phase shift and intensity modulation of luminescence following intensity-modulated excitation are measured as a function of modulation frequency and they are fitted into a double exponential decay. The fast decay component, compared with the slow one, has narrower spectral bandwidth and is emitted from the Eu^{3+} that has more polar and definite environment with higher symmetry and that interacts more easily with hydrated water molecules. The fast decay component is attributed to Eu^{3+} at site II' while the slow one to Eu^{3+} at sites I' and I.

Introduction

Zeolite molecular sieves have been widely studied[1-5] since they play indispensible roles in many technologically and economically important applications. The interactions of zeolites with encapsulated chemical species[4-7] are drastically different from those of solutions since zeolites have well-defined structures and various unusual catalytic effects.[8-11] Many of their catalytic properties are related to acidic and basic properties which depend on the types as well as amount of cations present in a zeolite.[2,3] The modification of zeolites by ion exchange of exchangeable cations[12,13] provides a useful means of tailoring their properties to particular applications. In particular, ion exchanges with rare-earth cations are reported to improve the thermal stability and catalytic activity of zeolites.[2,12,14] Improvement can be optimized by understanding the environment of cation binding sites and the interactions of lanthanide cations with their neighbors.

On the condition that materials or systems to be investigated contain a luminescent chromophore, its intrinsic luminescence can be taken advantage of to gain information on the structures, dynamics, or compositions of the objects.[15-19] Especially, rare-earth cations have been extensively employed to solve a variety of structural and analytical problems owing to their highly luminescent properties.[15,20-24] Their luminescence spectra, quantum yields, and lifetimes are very sensitive to their environmental changes. With this view Eu(III) luminescence is a particularly valuable probe. As seen in the schematic energy levels of aqueous Eu^{3+} in Figure 1, excitation to a strongly allowed state $^5L_6$ from the ground electronic state $^7F_0$ leads Eu^{3+} ion to $^5D_0$ state by means of fast nonradiative relaxation processes at room temperature, prior to radiative relaxation to one of ^7F_J (J=0 to 6) states. The monitored luminescence bands in this report are the transition bands of $^5D_0 \rightarrow {}^7F_1$ and $^5D_0 \rightarrow {}^7F_2$ and they will be called F_1 and F_2 respectively.

Although time-resolved luminescence techniques have been generally used in chemical, physical and biological researches, data are most commonly obtained by measuring time-dependent emission which follows excitation with a short pulse of light from a laser. However, time-domain luminescence spectroscopy is costly to introduce by reason of high-priced pulse laser and time-resolvable detector and it often requires tricky skills to take advantage of. Instead we employ a frequency-domain time-resolved luminescence technique in this experiment. The technique can be easily set up with a small budget and introduced even with a slight modification of a preexisting static luminescence spectrometer. It is also simple to use and maintain the spectrometer. The pulsed excitation source in time-domain spectroscopy is replaced with an intensity-modulated light source in this technique.[25-27] Because of the time lag between absorption and emission, emission is delayed in time relative to modulated excitation. At each modulation frequency this delay is expressed as the phase shift (ϕ) and modulation (m) of emission relative to those of excitation light.[25,28] For a single exponential decay the phase and modulation are related to luminescence lifetime (τ) and modulation frequency (f) by:

$$\tan\phi = 2\pi f \tau \quad (1)$$

$$m = [1+(2\pi f\tau)^2]^{-1/2} \quad (2)$$

In this experiment the phase shift and intensity mo-

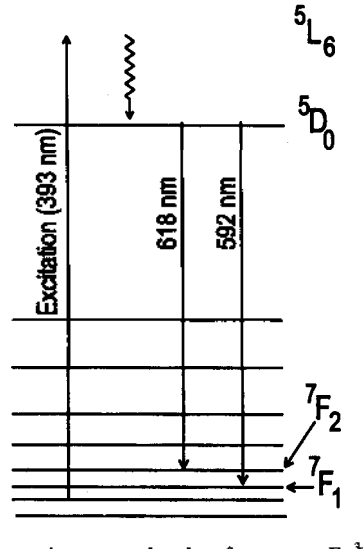

Figure 1. Schematic energy levels of aqueous Eu^{3+} to show the employed transitions for excitation and emission.

dulation of Eu(III) luminescence following intensity-modulated excitation are measured as functions of modulation frequency to characterize the surroundings of Eu^{3+} binding sites in Y zeolite and to understand the nature of Eu^{3+} ion interaction with neighbors. The results show that Eu(III) luminescence phase-modulation spectroscopy is an excellent probe into cation binding sites.

Experimental

Eu^{3+}-exchanged Y zeolite (EuY) was prepared by refluxing synthesized Na^+-exchanged Y zeolite (NaY) in stoichiometrically concentrated $EuCl_3$ aqueous solution at 70-80 °C for a day. Refluxed zeolite was filtered, dried in a desiccator overnight and then transferred into a glass-jointed quartz tube of 6-mm inner diameter under nitrogen atmosphere. The tubed sample was further-dehydrated and calcined at 400 °C under vaccum for 6 h until the glass entrance of the tube was sealed off with a torch. However, calcined sample still contains a great number of hydrated water molecules. Deuterated samples were prepared by treating the above refluxing procedure in ^2H_2O.

The employed phase shift luminometer is schematically shown in Figure 2. Sample excitation beam from a 350-W Xe lamp (Schoeffel, LPS 255HR) was dispersed using a 0.25-m monochromator (Kratos, GM 252) and modulated using an optical chopper (SRS, SR540). Luminescence was collected from the front surface of sample excitation and focused to a 0.275-m monochromator (ARS, Spectrapro-275) to which a photomultiplier tube (Hamamatu, R376) was attached. The luminescence intensity with its $\sin\phi$ and $\cos\phi$ values was measured as a function of wavelength by amplifying the photomultiplier signal with a lock-in analyzer (Ithaco, 393 Dynatrac 3). The phase shift and intensity modulation of luminescence were measured at various modulation frequencies and their actual values were carefully calculated after eliminating Eu^{3+}-independent background luminescence. All the spectroscopic results reported here were measured at room temperature.

Results and Discussion

The static Eu(III) luminescence spectrum of EuY zeolite (the one at f=0 in Figure 3) is quite different from that of Eu^{3+} aqueous solution. Spectral shifts are not noticeable with our current spectral resolution. However, the relative intensity of F_2 band increases dramatically with binding to zeolite and becomes even much larger than that of F_1 band. The electric dipole transition of F_2 is forbidden by parity in a symmetry with an inversion center such as octahedral group.[29,30] However, interactions with the ligand field or with vibrational states mix electronic states of different parities and the transition[29,31] arising from this state hybridization is called forced electric dipole transition. Since the forced transition of F_2 is originating from interactions with neighbors, it is so hypersensitive to environment as to be employed frequently to probe environmental, especially short range, effect on the centered Eu^{3+} ion.[32,33] At the same time the magnetic dipole transition of F_1 is allowed and insensitive to the stark effect caused by local ligand field. For this reason F_1 transition is usually utilized as an internal standard in monitoring the surroundings of Eu^{3+} ion.[31,34] For example, if RI(2), the ratio of F_2 luminescence intensity to F_1 intensity, is larger, the binding site of Eu^{3+} ion has lower symmetry and less polar and more covalent characters.[31] The RI(2) value of Y zeolite is as large as 4 while that of aqueous solution is 0.6. This indicates that the Eu^{3+} sites of Y zeolite have much lower symmetry and less polar and more covalent characters than water. In particular, the large value of RI(2) unquestionably designates that the symmetries of Eu^{3+} binding sites are significantly lower than octahedral group. Although it is not apparent to notice with the signal-to-noise ratios and unnormalized plots of Figure 3, the Eu(III) luminescence spectrum of EuY becomes smaller in the spectral bandwidth of F_2 transition and in the value of RI(2) as the excitation modulation frequency increases. These indicate that the luminescence is emitted from at least two different sites. The luminescence with a longer lifetime is demodulated to a greater extent, so that its percent intensity lessens with the increment of modulation frequency. Examining the spectral change with modulation frequency, we can separate environmentally hypersensitive F_2 bands originated from different locations and discuss the different environments of Eu^{3+} binding places later.

Figure 4 illustrates the phase shift and intensity mo-

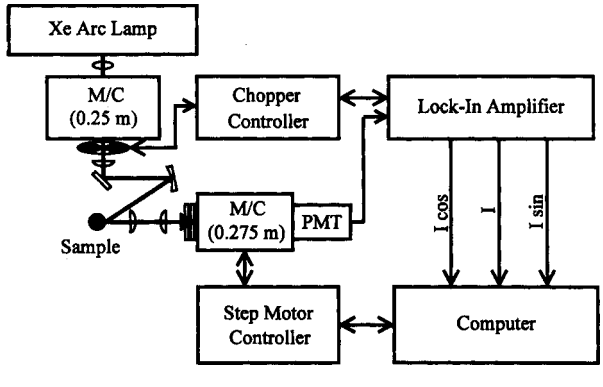

Figure 2. Schematic setup of phase luminometry.

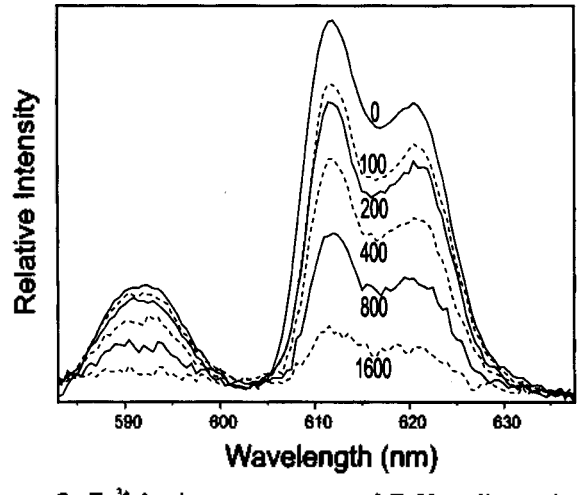

Figure 3. Eu^{3+} luminescence spectra of EuY zeolite excited at 393 nm, showing f-dependent luminescence intensity demodulation. The numbers adjacent to spectra are respective excitation modulation frequencies.

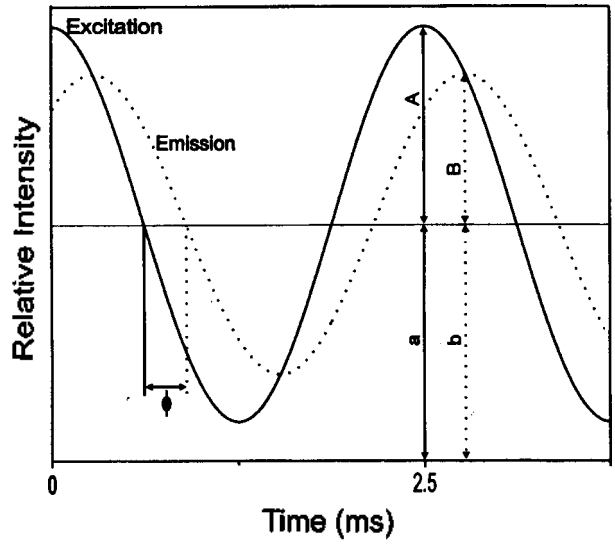

Figure 4. Illustrated phase modulation of F_1 luminescence from EuY in response to the intensity-modulated excitation of 393-nm light at 400 Hz. At this modulation frequency the time lag between absorption and emission results in the phase shift of 40° and the emission modulation of 0.76.

dulation of F_1 luminescence in response to excitation intensity modulation at 400 Hz. The emission of luminescence is delayed in time relative to the absorption of modulated excitation light because of the time lag between absorption and emission. As the result of this time delay, the phase of luminescence is shifted 40° from that of excitation while luminescence modulation, m=(B/A)/(b/a) in Figure 4, is reduced to 0.76 at the modulation frequency of 400 Hz in the phase-modulation spectroscopy of Eu(III) luminescence from EuY zeolite. The modulation decreases but the phase shift increases with increasing modulation frequency (Figure 3 and Table 1), as we know that ϕ and m change from 0° and 1.0 to 90° and 0.0, respectively, with the increase of f. However, the lifetime calculated using ϕ or m should remain invariable regardless of f within the experimental errors if luminescence has a single exponential decay.[26] Then the modification of the apparent lifetime presented in Table 1 with the variation of f suggests that luminescence has more than one decay components.

Figure 5 shows that the intensity modulations of Eu(III) luminescence from EuY fit well into a double exponential decay, yielding the time constants of 150 (52%) and 590 (48%) μs. Since luminescence components with different time constants are expected to originate from different environments, we have tried to understand individual sur-

Table 1. Modulation spectroscopic results of Eu^{3+} luminescence from EuY zeolite

f (s^{-1})	m[a]	ϕ[a] (degree)	τ_{obs}[b] (ms)
0	1.0	0	–
100	0.97	14	0.39
200	0.90	26	0.39
400	0.76	40	0.34
800	0.57	56	0.29
1600	0.37	68	0.25

[a] Both m and ϕ are calculated from f-dependent intensity modulations of F_1 luminescence. [b] τ_{obs}, $(1-m^2)^{1/2}/(2\pi fm)$, is apparent luminescence lifetime at a given f.

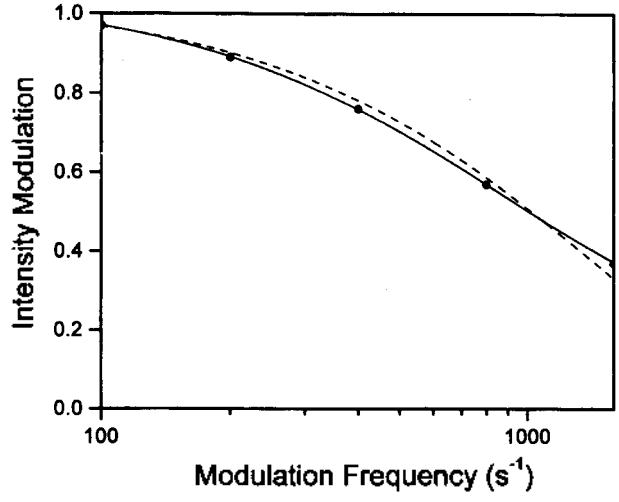

Figure 5. The best single (dotted) and double (solid) exponential decay fits of observed F_1 intensity modulations measured at various modulation frequencies. The double decay fit gives birth to 150 (52%) and 590 (48%) μs while the single one yields 270 μs.

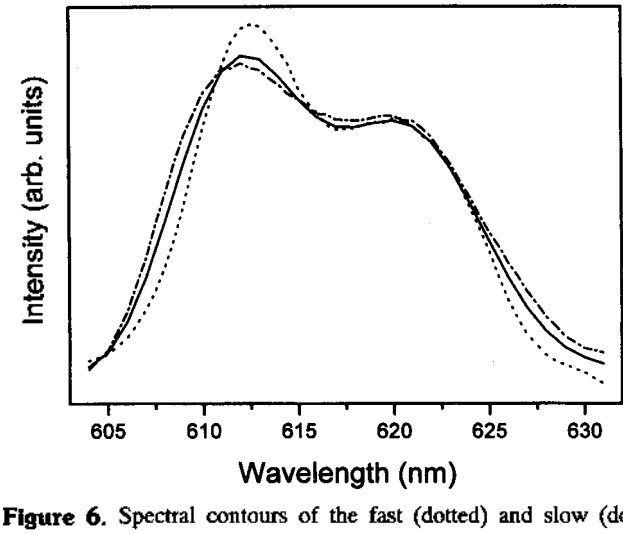

Figure 6. Spectral contours of the fast (dotted) and slow (dot-and-dashed) decay components separated from a raw F_2 band (solid). The separation procedures are described in the text. The band width of the fast component is surely narrower than that of the slow one.

Table 2. Variations of decay time constants with hydrogen isotope exchange and water coordination numbers calculated from these variations

Component Name	Refluxed in ^1H_2O		Refluxed in ^2H_2O		Water Coordination Number[b]
	τ (μs)	Amplitude[a]	τ (μs)	Amplitude	
fast	150	52%	340	52%	3.7
slow	590	48%	910	48%	0.6

[a] The percent amplitudes were measured from F_1 luminescence and [b] the numbers of coordinated water molecules were calculated following the ref. 35.

roundings by measuring decay time variations with hydrogen isotope exchange[35,36] and by separating the F_2 bands of two decay components spectrally. The fast and slow decay time constants of 150 and 590 μs are altered into 340 and 910 μs respectively, without showing considerable changes in relative amplitude, as hydrated water, residually existing in the surface of calcined EuY zeolite sample, is exchanged with heavy water. The numbers of water molecules coordinated to Eu^{3+} ion, calculated following the method of the ref. 35, are 3.7 and 0.6 for the fast and slow decay components, respectively. Considered that aqueous Eu^{3+} ion has 8 to 9 coordinated water molecules in the aspect of Eu(III) luminescence quenching dynamics,[35,37] the actual numbers of coordinated water molecules might be lower than the observed ones. Nevertheless, we can suggest that the Eu^{3+} site responsible for the fast decay is located much closer to hydrated water molecules than the site for the slow one.

As briefly mentioned early, F_2 spectral bandwidth and RI (2) in Figure 3 decrease with modulation frequency increment. This suggests that the spectral bandwidth and RI(2) of the fast component are smaller than those of the slow one, for the slow decaying luminescence is demodulated more drastically so that the relative intensity of the fast one augments with f increment. In order to inspect the spectral difference between the fast and slow decay components we have tried to separate the spectral contours of the two components by intermixing the spectra at 0 and 1600 Hz in Figure 3 linearly. After the F_2 bands of both spectra were smoothed, the one at 1600 Hz was multiplied by a factor and subtracted from the one at 0 Hz, which we call the raw band, to make the residual band, which we call the slow (decaying component's F_2) band, different from the F_2 band at 1600 Hz as much as possible. Then the slow band was multiplied by a factor and subtracted from the raw band to make this new residual band, which we call fast (decaying component's F_2) band, distinct from the slow band as much as possible. Compared with the slow band, the fast band has narrower bandwidth and smaller RI(2) and is shifted to the red. The smaller RI(2) suggests that the fast band is emitted from more ionic environmental site with higher symmetry, although the sites yielding both fast and slow bands are much less symmetric and polar than water. The narrower bandwidth signifies more definite location for fast decaying luminescence. In other words the slow decaying luminescence is brought about by more than one sites with slightly different characters in fact, even though they are called the slow component's site. The overall red shift also implies more polar environment for the fast band.

Compared with the slow decaying luminescence, the fast one originates from more ionic environment and well-defined location with higher symmetry. The Eu^{3+} ion attributed to the fast one has more coordinated water molecules, indicating closer location to the hydrated surface of supercage. Combining the observed results together, we allocate the site II' for the location of Eu^{3+} emitting the fast one and the sites I' and I for the locations of Eu^{3+} emitting the slow one. Metal cations in Y zeolite are reported[2,13,38] to migrate from supercage to sodalite cage or hexagonal prism irreversibly during dehydration process. The cation binding site in hexagonal prism is called site I. However there are two cation sites in sodalite cage, one of which is near site I and called site I'. The other one is located close to supercage and named site II'. A unit cell of dehydrated La^{3+}-exchanged zeolite Y is reported[39] to have 13.1, 16.0, 29.1 La^{3+} ions at sites I, I', and II, respectively. The one stable location of site II agrees with the narrower spectral width of the fast component and two similar but different positions of sites I' and I go with the broader F_2 band of the slow component. The cation site of supercage near site II' is called site II and it contains 30 Na^+ for each unit cell of dehydrated NaY zeolite, while sites I and I' bear 7.5 and 19.5 Na^+ ions respectively. The more ionic environment of site II' also goes well with the smaller RI(2) and red shift of the fast component. Much easier interaction of excited Eu^{3+} at site II' with water molecules hydrated at the polar location of site II was suggested as well by the larger water coordination number of the fast component.

These introductory Eu(III) phase luminometric results in Y zeolite exhibit that simple phase-modulation Eu(III) luminescence spectroscopy, easy to introduce with a small budget and convenient to utilize, is an excellent site-selective probe into metal cation surroundings. Important results in this study are summarized as follows. Eu(III) luminescence in Y zeolite has a large RI(2), revealing that Eu^{3+} sites have much lower symmetry and less polarity than water. It decays with two time constants of 150 and 590 μs. The fast component, compared with the slow one, exhibits red-shifted F_2 band with narrower bandwidth and smaller RI (2), implying relatively more ionic and well-defined location with higher symmetry. More coordinated waters designate that Eu^{3+} giving birth to the fast one is located closer to hydrated waters in the supercage. These observations collectively suggest to ascribe the fast one to the site II' and the slow one to the sites I' and I.

Acknowledgment. We thank Professor Ryong Ryoo at the Center for Molecular Science for his kind gift of Y zeolite. This work was supported by the grant 961-0305-083-2 of the Korea Science and Engineering Foundation. We also acknowledge the Korea Ministry of Education for partial financial support.

References

*Also a member of the Center for Molecular Science, Taejon 305-701, Korea.

1. Chen, W.; Wang, Z. G.; Lin, Z. J.; Lin, L. Y. *Solid State Commun.* **1997**, *101*, 371.
2. Gaare, K.; Akporiaye, D. *J. Phys. Chem. B* **1997**, *101*, 48.
3. Takatani, S.; Fukumura, H.; Masuhara, H. *J. Phys. Chem. B* **1997**, *101*, 3365.
4. Kao, H.-M.; Grey, C. P. *J. Phys. Chem.* **1996**, *100*, 5105.
5. Kassab, E.; Fouquet, J.; Allavena, M.; Evleth, E. M. *J. Phys. Chem.* **1993**, *97*, 9034.
6. Cizmeciyan, D.; Sonnichsen, L. B.; Garcia-Garibay, M. A. *J. Am. Chem. Soc.* **1997**, *119*, 184.
7. Park, J.; Kang, W.-K.; Ryoo, R.; Jung, K.-H.; Jang, D.-J. *J. Photochem. Photobiol. A: Chem.* **1994**, *80*, 333.
8. Yoon, K. B.; Park, Y. S.; Kochi, J. K. *J. Am. Chem. Soc.* **1996**, *118*, 12710.
9. Ramamurthy, V. *J. Am. Chem. Soc.* **1994**, *116*, 1345.

10. Ramamurthy, V.; Sanderson, D. R.; Eaton, D. F. *J. Phys. Chem.* **1993**, *97*, 13380.
11. Kang, W.-K.; Cho, S.-J.; Lee, M.; Kim, D.-H.; Ryoo, R.; Jung, K.-H.; Jang, D.-J. *Bull. Korean Chem. Soc.* **1992**, *13*, 140.
12. Hong, S. B.; Shin, E. W.; Moon, S. H.; Pyun, C.-H.; Kim, C.-H.; Uh, Y. S. *J. Phys. Chem.* **1995**, *99*, 12274.
13. Baker, M. D.; Olken, M. M.; Ozin, G. A. *J. Am. Chem. Soc.* **1988**, *110*, 5709.
14. Bada, T.; Hikita, S.; Ono, Y.; Yoshida, T.; Tanaka, T.; Yoshida, S. *J. Mol. Cat. A: Chem.* **1995**, *98*, 49.
15. Yamase, T.; Kobayashi, T.; Sugeta, M.; Naruke, H. *J. Phys. Chem. A* **1997**, *101*, 5046.
16. Gfeller, N.; Calzaferri, G. *J. Phys. Chem. B* **1997**, *101*, 1396.
17. Wolbers, M. P. O.; van Veggle, F. C. J. M.; Snellink-Ruël, B. H. M.; Hofstraat, J. W.; Geurts, F. A. J.; Reinhoudt, D. N. *J. Am. Chem. Soc.* **1997**, *119*, 138.
18. Mirochnik, A. G.; Petrochenkova, N. V.; Karasev, V. E. *Russian Chem. Bull.* **1996**, *45*, 1356.
19. Prodi, L.; Maestri, M.; Ziessel, R.; Balzani, V. *Inorg. Chem.* **1991**, *30*, 3798.
20. Fujita, K.; Tanaka, K.; Hirao, K.; Soga, N. *J. Appl. Phys.* **1997**, *81*, 924.
21. Pucker, G.; Catterer, K.; Fritzer, H. P.; Bettinelli, M.; Ferrari, M. *Phys. Rev. B* **1996**, *53*, 6225.
22. Tanaka, T.; Yoshida, T.; Yoshida, S.; Baba, T.; Ono, Y. *Physica B* **1995**, *208&209*, 687.
23. Rizk, M.; El-Shabrawy, Y.; Zakhari, N. A.; Toubar, S. S.; Carreira, L. A. *Spectrosc. Lett.* **1995**, *28*, 1235.
24. Reuben, J. *Handbook on the Physics and Chemistry of Rare Earths*; North-Holland Publishing Company: 1979; p 515.
25. Jameson, D. M.; Weber, G. *J. Phys. Chem.* **1981**, *85*, 953.
26. Gratton, E.; Limkeman, M. *Biophys. J.* **1983**, *44*, 315.
27. Lakowicz, J. R.; Laczko, G.; Gryczynski, I.; Cherek, H. *J. Biol. Chem.* **1986**, *261*, 2240.
28. Weber, G. *J. Phys. Chem.* **1981**, *85*, 949.
29. Bunzli, J.-C. G.; Choppin, G. R. *Lanthanide Probes in Life, Chemical and Earth Sciences*; Elsevier Science: Amsterdam, The Netherlands, 1989; p 219.
30. Bergaya, F.; van Damme, H. *J. Chem. Soc., Faraday Trans.* **1983**, *79*, 505.
31. Oomen, E. W. J. L.; van Dongen, A. M. A. *J. Non-Cryst. Sol.* **1989**, *111*, 205.
32. Carlos, L. D.; Videira, A. L. L. *Phys. Rev. B* **1994**, *49*, 11721.
33. Richardson, F. S. *Chem. Rev.* **1982**, *82*, 541.
34. Levy, D.; Reisfeld, R.; Avnir, D. *Chem. Phys. Lett.* **1984**, *109*, 593.
35. Horrocks, Jr., W. DeW.; Subnick, D. R. *Acc. Chem. Res.* **1981**, *14*, 384.
36. Haas, Y.; Stein, G. *J. Phys. Chem.* **1972**, *76*, 1093.
37. Horrocks, Jr., W. DeW.; Subnick, D. R. *J. Am. Chem. Soc.* **1979**, *101-2*, 334.
38. Iton, L. E. *J. Phys. Chem.* **1977**, *81*, 435.
39. Breck, D. W. *Zeolite Molecular Sieves: Structure, Chemistry, and Use*; John Wiley & Sons: U.S.A., 1974; p 100.

The Interaction of Chiral Amino Thiols with Organozinc Reagents and Aldehydes: A Mechanism of Amino Thiol-Catalyzed Addition of Organozinc Reagents to Aldehydes

Jahyo Kang*, Jin Bum Kim, Jeeyoung Kim, and Duckhwan Lee*

Department of Chemistry, Sogang University, Seoul 121-742, Korea
Received February 4, 1998

Details of various equilibria involved in the reactions of oxaza- and thiazazincolidine catalysts, generated from either β-amino alcohol or β-amino thiol, with aldehyde were studied by colligative measurements. The results indicated that the coordination of diethylzinc prior to the coordination of aldehyde is essential for high enantioselectivity of the thiol catalyzed reaction. The probable origin of asymmetric nonlinearity is also presented.

Introduction

The β-amino alcohol catalyzed addition of dialkylzinc reagents to aldehydes is quite general for preparation of optically active secondary alcohols, for which extensive mechanistic studies have been carried out by many groups.[1,2] We have also developed chiral cyclic amino *thiols*, especially piperidine compound **1** derived from commercially available enantiopure norephedrine, which have turned out to be an excellent ligand for thiazazincolidine catalyst. The thiol ligands were expected to be highly effective due to the fact 1) the sulfur in thiol is more easily polarizable compared to the oxygen in alcohol, 2) the heterocyclic ring may become a face blocker, 3) the thiol and thiolates have higher affinity toward metals, especially zinc, and 4) the metal thiolates have less tendency of diminishing the Lewis